CISTER
Research Centre in
Real-Time & Embedded
Computing Systems

Journal Paper

Joint Beamforming, Terminal Scheduling, and Adaptive Modulation with Imperfect CSIT in Rice Fading Correlated Channels with non-persistent Co-channel Interference

Ramiro Robles

CISTER-TR-171103

2018

Joint Beamforming, Terminal Scheduling, and Adaptive Modulation with Imperfect CSIT in Rice Fading Correlated Channels with non-persistent Co-channel Interference

Ramiro Robles

*CISTER Research Centre

Polytechnic Institute of Porto (ISEP-IPP)

Rua Dr. António Bernardino de Almeida, 431

4200-072 Porto

Portugal

Tel.: +351.22.8340509, Fax: +351.22.8321159

E-mail: rasro@isep.ipp.pt

http://www.cister.isep.ipp.pt

Abstract

This paper presents a resource allocation algorithm for multi-user wireless networks affected by non-persistent co-channel interference. The analysis considers a network with one base station (BS) that uses a multiple antenna transmitter (beamformer) to schedule (in a time-division manner) transmissions towards a set of J one-antenna terminals in the presence of K non-persistent interferers. The transmitter is assumed to employ Maximum-Ratio Combining (MRC) beamforming with spatially-correlated branches and channel envelopes modelled as Rice-distributed processes. The BS has access to an imperfect (outdated) copy of the instantaneous Channel State Information (CSI) of each terminal. Based on this CSI at the transmitter side (CSIT), the BS proceeds to select (at each time interval or time-slot) the terminal with the highest measured channel strength for purposes of transmission. This imperfect CSIT is also used to calculate the coefficients of the beamformer that will be used to transmit information towards the scheduled terminal, as well as for selecting the most appropriate modulation format (via threshold-based decision). The main merits of this work are the following: 1) joint analysis of MRC-based beamforming, terminal scheduling based on maximum channel strength, and modulation assignment, and 2) joint modelling of the effects of spatial correlation, co-channel interference and imperfect CSIT. Results suggest that scheduling helps in rejecting co-channel interference and the degrading effects of imperfect CSIT. Spatial correlation could some times lead to better performance than the uncorrelated case, particularly in the low SNR (Signal-to-Noise Ratio) regime. Conversely, uncorrelated branches always outperform the correlated case in the high SNR regime. Spatial correlation tends to accumulate over the antenna array thus leading to a more noticeable performance degradation and more allocation errors due to the outdated CSIT assumption. The line of sight component is found to contribute to a better reception, but it also reduces the ability to counteract the degrading effects of imperfect CSIT due to the lack of diversity combining.

Joint Beamforming, Terminal Scheduling, and Adaptive Modulation with Imperfect CSIT in Rice Fading Correlated Channels with non-persistent Co-channel Interference

Ramiro Sámano-Robles

Research Centre in Real-time and Embedded Computing Systems
Instituto Politécnico do Porto, Porto, Portugal
Email: rasro@isep.ipp.pt

Abstract*—This paper presents a resource allocation algorithm for multi-user wireless networks with non-persistent co-channel interference. The analysis considers a network with one base station (BS) that employs an N multiple antenna transmitter (beamformer) to schedule (in a time-division format) a set of J one-antenna terminals in the presence of K non-persistent interferers. The transmitter is assumed to employ Maximum-Ratio Combining (MRC) beamforming with spatially-correlated branches and channel envelopes modelled as Rice-distributed processes. The BS has access to an imperfect (outdated) copy of the instantaneous Channel State Information (CSI) of each terminal. Based on this CSI at the transmitter side (CSIT), the BS proceeds to select (at each time interval or time-slot) the terminal with the highest measured channel strength. This imperfect CSIT is also used to calculate the coefficients of the beamformer that will be used to transmit information towards the scheduled terminal, as well as for selecting the most appropriate modulation format (via threshold-based decision). The main merits of this work are the following: 1) joint analysis of MRC-based beamforming, terminal scheduling based on maximum channel strength, and modulation assignment, and 2) impact analysis of spatial correlation, line-of-sight (LOS), co-channel interference, and imperfect CSIT. Results suggest that maximum channel strength scheduling helps in rejecting co-channel interference and the degrading effects of imperfect CSIT (due to multi-user diversity gains). Spatial correlation could some times lead to better performance than the uncorrelated case, particularly in the low SNR (Signal-to-Noise Ratio) regime. Conversely, uncorrelated branches always outperform the correlated case in the high SNR regime. Spatial correlation tends to accumulate over the antenna array thus leading to a more noticeable performance degradation and more allocation errors due to the outdated CSIT assumption. The LOS channel component is found to contribute to a better reception in general, but it also reduces the ability to counteract the degrading effects of imperfect CSIT due to the lack of diversity combining gains.

Keywords–Beamforming; Scheduling; Resource allocation; Imperfect CSIT; Maximum Ratio Combining (MRC).

I. INTRODUCTION

Multiple antenna systems (also known as MIMO or Multiple-Input Multiple-Output systems) are expected to proliferate in the coming years, particularly in the context of 5G or fifth-generation of wireless systems [1][2]. The growing demand for wireless connectivity, the limited transmission resources, and the outdated spectrum allocation paradigm have created the need for more efficient, scalable and higher capacity transmission systems. MIMO technology offers considerable capacity growth that escalates with the number of transmit-receive antenna pairs (see [3] for an overview of capacity in MIMO channels). MIMO also offers improved energetic efficiency and reduced interference with minimum spectrum expenditure.

From the many different types of multiple antenna systems, perhaps *beamforming* technology represents the option with higher potential for commercial implementation, mainly due to its maturity, flexible implementation, and low computational costs (in comparison with other MIMO solutions). Beamforming refers to the ability to dynamically steer the phases of an antenna array and change the directionality properties of the resulting radiation beams. This enables a wide set of applications in multi-user settings, such as: interference rejection/management [4], spatial multiplexing [5], and more recently (with a few modifications) 3D beamforming with massive MIMO in 5G [6], beam-division multiple access [7], and interference alignment [8]. Other works in beamforming can be found in [9]-[11]. In future networks, beamforming will be key for efficiently organizing spectrum resources in dense cooperative small cells, as well as minimizing energy expenditure, reducing leakage and/or interference to adjacent cells or terminals, and also for improving security against potential attacks of signal jamming or eavesdropping in the network.

All these advances in the PHYsical (PHY) layer of multiple antenna systems need to be integrated/optimised with upper-layer algorithms, particularly with radio resource management (see [12]-[18]). This has opened several issues regarding the cross-layer design and optimization of beamforming and in general multiple-antenna systems. One particularly important topic in this field is the modelling of the underlying multiple antenna signal processing tools to be used in resource allocation and system-level evaluation frameworks. In large network set ups with tens or hundreds of BSs and hundreds or thousands of terminals, all the parameters of the PHY-layer cannot be usually included in full detail in the analysis or system-level simulation loop. Therefore, a trade-off must be found between the accuracy of the model that represents the underlying PHY-layer and its flexibility for purposes of resource allocation and optimisation at the system-level.

This paper attempts to partially fill these gaps by addressing the link-layer interface modelling in Rice fading correlated channels of an *adaptive wireless multi-user network using Maximum-Ratio Combining (MRC) beamforming and terminal scheduling based on limited (outdated) feedback*. The transmitter selects the most adequate Modulation and Coding Schemes (MCSs) and beamforming vectors based on an estimated Channel State Information (CSI). This imperfect CSI at the transmitter side (i.e., CSIT) is assumed to have been initially collected by the receiver (perfect estimation), and subsequently reported back to the transmitter via a feedback channel affected by delay (outdated information). This paper presents the analysis of the statistics of correct reception process conditional on the decision made by the transmitter (*modulation format selection, beamforming and scheduling*) based on the inaccurate CSIT. Link-layer throughput is evaluated by means of an *interface model* based on an instantaneous Signal-to-Interference-plus-Noise Ratio (SINR) adaptive switching threshold scheme for modulation assignment. This model aims to provide an accurate but flexible representation of the underlying PHY-layer suitable for upper-layer design. In the proposed model, a packet transmission using a given MCS is considered as correctly received with given values of BLock-Error Rate (BLER) and spectral efficiency whenever the instantaneous SINR exceeds the reception threshold of the selected MCS. The reception parameters of each MCS are obtained from Look-Up-Tables (LUTs) previously calculated via *off-line PHY-layer simulation*. The main contribution of this work is the joint analysis of spatial correlation, imperfect CSIT and non-persistent co-channel interference in link adaptation and terminal scheduling for MRC-based multiple antenna beamforming systems. This paper constitutes an extension of the work in the conference paper in [1] from Rayleigh channel to include a line-of-sight (LOS) channel component, i.e., Rice channel assumption. This paper also extends the conference paper from persistent channel interferers to non-persistent ones, which matches better real life settings where co-channel systems operate under randomized traffic distributions.

This paper is organized as follows. Section II describes previous works and the achievements of this paper with respect to the state of the art. Section III describes the system model and the assumptions of the paper. Section IV presents the link-layer interface model. Section V deals with the statistics of the estimated SNR and the instantaneous SINR. Section VI presents analytic results and sketches of the statistics of packet reception using different network assumptions. Finally, Section VII presents the conclusions of this paper.

II. Previous works

In theory, the simplest multiple antenna system is the MRC transceiver, which provides a relatively flexible framework for statistical analysis, interface modelling, and resource management. The literature of MRC transceivers has focused on the derivation of outage and bit error probability distributions (see [19]-[27]). The effects of imperfect channel knowledge on the performance of MRC receivers in Rayleigh fading correlated channels can be found in [19]-[20] following the analysis with perfect channel estimation presented in [21]. A series expansion of the statistics of MRC systems with correlated Rician channels is given in [22]. A unified approach for analysis of two-stage MRC systems with hybrid selection in generalized Rice correlated channels was proposed in [23]. Extensions to the case of co-channel interference are given in [24]-[27].

The present work considers the extension of outage probability analysis of MRC transmitters (beamformers) to the study of Adaptive Modulation and Coding (AMC) in Rice fading correlated channels with imperfect/outdated CSIT and no-persistent co-channel interference. To the best of our knowledge, this is the first attempt in the literature that addresses these issues under the same framework. This work attempts to extend the analysis of MRC systems towards including resource allocation aspects which are typical of upper layer design (radio resource management). In addition, network design and in particular resource allocation for multiple antenna systems is usually conducted under the assumption perfect CSIT. Imperfect CSIT has been addressed in [28] for distributed systems and in [29] for energy efficient MIMO link adaptation. In comparison with these works, which are focused on numerical evaluation of imperfect CSIT, this work provides an analytic framework for obtaining the statistics of errors in MCS assignment for correlated MRC transmitters.

The work in [30] provides a review of the state of the art of limited feedback in adaptation schemes for MIMO systems. The work in [31] presents the analysis of adaptive modulation for two-antenna beam-formers considering mean CSI at the transmitter side. The work in [32] addressed the impact of outdated feedback on AMC and user selection diversity systems for MIMO systems in Rayleigh uncorrelated channels. Other works with limited feedback for different types of system can be found in [34]-[36]. All these previous works consider uncorrelated MIMO channels. This work goes beyond this assumption searching for a joint analysis of limited feedback and spatial correlation for adaptive MRC transmitters with non-persistent co-channel interference.

Notation: Bold lower case letters (e.g., $\mathbf{x}$) denote vector variables, bold upper case letters (e.g., $\mathbf{A}$) denote matrices, $(\cdot)^T$ is the vector transpose operator, $(\cdot)^H$ is the Hermitian transpose operator, $E[\cdot]$ is the statistical average operator, $(\cdot)^*$ is the complex conjugate operator, f_z, F_z and $\bar{F}_z$ denote, respectively, the Probability Density Function (PDF), Cumulative Density Function (CDF) and Complementary Cumulative Density Function (CCDF) of any random variable z, $Re(\cdot)$ denotes the real part operator, and $\left(\begin{array}{c} J-1 \\ \mathbf{l} \end{array}\right) = \left(\begin{array}{c} J-1 \\ l_0, l_1, \dots l_L \end{array}\right) = \frac{(J-1)!}{l_0! l_1!, \dots l_L}$ is the multinomial combinatorial number of $J-1$ and $L+1$ coefficients $l_0, l_1, \dots l_L$ arranged in the vector $\mathbf{l} = [l_0, l_1, \dots, l_L]^T$.

III. System model and assumptions

Consider the network depicted in Figure 1 with one Base Station (BS) scheduling transmissions (in a time-division fashion) towards J terminals , each one with one receiving antenna, and a set of K non-persistent single-antenna interferers. The BS uses an N-antenna Maximum-Ratio Combining (MRC) beamformer that is used to transmit information to a given terminal at specific time slots. The channel vector between the BS and the jth terminal is denoted by $\mathbf{h}_j = [h_j(1), h_j(2), \dots h_j(N)]^T$. All instantaneous channel variables will be modelled as non-zero-mean complex circular Gaussian random variables with variance γ and mean ν: $h_j(n) \sim \mathcal{CN}(\nu, \gamma)$. The estimated channel variable available at the transmitter side is given by $\hat{\mathbf{h}}_j = [\hat{h}_j(1), \hat{h}_j(2), \dots \hat{h}_j(N)]^T$. This information is used by the BS for purposes of beamforming, terminal scheduling and resource allocation (modulation format assignment). The channel between the interferer k towards terminal j is denoted by $h_{k,j}$ and is also modelled as a non-zero-mean complex circular Gaussian random variable with variance λ: $h_{k,j} \sim \mathcal{CN}(\xi, \lambda)$. It is assumed that the transmissions of the interferers are controlled by a binary Bernoulli random process δ_k described by the parameter p: $p = \Pr\{\delta_k = 1\}$.

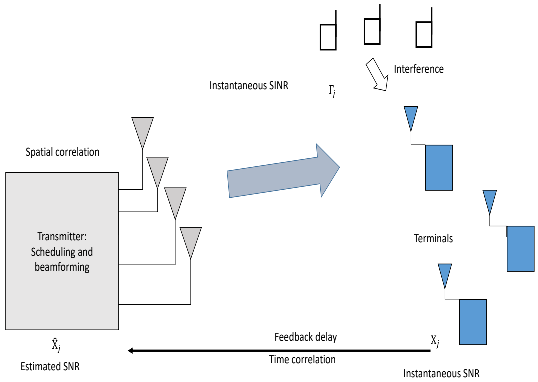

Figure 1. Wireless network with one transmitter using imperfect CSIT for scheduling, modulation assignment and beamforming information to a set of terminals in the presence of co-channel interference.

TABLE I. LIST OF VARIABLES.

Variable	Meaning
N	Number of antennas at the transmitter side
ρ	Spatial correlation coefficient
ρ_c	Temporal correlation coefficient
P	Transmit power
σ_v^2	Noise variance
γ	Channel variance
λ	Interferer channel variance
J	Number of terminals
M	Number of modulation formats
$\mathbf{h}_j$	Channel vector of terminal j
$\mathbf{w}_j$	Beamforming vector for terminal j
$\hat{\mathbf{h}}_j$	Estimated channel vector
$\hat{X}_j$	Estimated SNR for terminal j
Γ_j	Instantaneous SINR of terminal j
I_j	Interference experienced by terminal j
$h_{k,j}$	Channel between interferer k and terminal j
ν	Line of sight component main link
ξ	Line of sight component interfere link
K	Number of non-persistent interferers
s_j	Symbol transmitted towards terminal j
$\check{s}_k$	Symbol transmitted by interferer k
β_m	Reception SINR target threshold for modulation format m
θ_m	BLER for modulation format m @ β_m
η_m	Spectral efficiency of modulation format m @ β_m
T	Link Layer throughput
$\hat{\beta}_m$	Selection SNR threshold of modulation format m
δ_k	transmission binary control variable for interferer k
p	Interferer random transmission persistent factor

For each terminal, the BS selects one of M modulation formats, which are arranged in increasing order according to their target Signal-to-Interference plus Noise Ratio (SINR). The target SINR of the mth MCS will be denoted by β_m. The variables θ_m and η_m will denote, respectively, the BLER and spectral efficiency (in bps/Hz) considering operation at the target SINR of the mth MCS. It is assumed that the receiver monitors the quality of the channel and reports it back to the transmitter. Based on this collected Channel State Information (CSI), the transmitter selects the most appropriate MCS using a correction for the decision thresholds denoted here by $\hat{\beta}_m$. This paper considers perfect channel estimation at the receiver side and imperfect channel state information at the transmitter side (CSIT). Imperfect CSIT is assumed to be mainly due to a feedback channel affected by delay. The beamforming vector is denoted by $\mathbf{w}_j = [w_j(1), w_j(2), \ldots, w_j(N)]^T$, which using the MRC criterion is given by $\mathbf{w}_j = \mathbf{h}_j^*$. Therefore, the signal received by the scheduled terminal can be mathematically written as follows

$$r_j = \mathbf{w}_j^T \mathbf{h}_j s_j + \sum_{k=1}^{K} \delta_k h_{k,j} \check{s}_k + v_j, \quad (1)$$

where s_j is the information symbol transmitted towards terminal j, $\check{s}_k$ is the symbol transmitted by interferer k, δ_k is the binary random variable that controls the transmissions of the non-persistent interferers ($p = \Pr\{\delta_k = 1\}$), and v_j is the additive white Gaussian noise experienced by terminal j with variance σ_v^2: $v_j \sim \mathcal{CN}(0, \sigma_v^2)$. Considering the symbol transmit power constraint $E[s_j^* s_j] = P$, the estimated SNR at the transmitter side from (1) is given by:

$$\hat{X}_j = \frac{\hat{\mathbf{h}}_j^H \hat{\mathbf{h}}_j E[s_j^* s_j]}{\sigma_v^2} = \frac{\sum_{n=1}^{N} P|\hat{h}_j(n)|^2}{\sigma_v^2}. \quad (2)$$

Note that in this paper it is assumed that an estimate of interference $I_j = \sum_{k=1}^{K} \delta_k h_{k,j} \check{s}_k$ in (1) is not available at the transmitter. Therefore, all decisions will be based on an estimate of the SNR in (2). The estimated channels will be generated using the following linear correlation model:

$$\hat{h}_j(n) = \nu + \sqrt{1-\rho} Z_j(n) + \sqrt{\rho} G_j = \nu + \hat{\phi}_j(n), \quad (3)$$

where ρ is the spatial correlation coefficient and the terms $Z_j(n)$ and G_j are the zero-mean complex circular Gaussian variables with variance γ. Considering that $h_j(n) = \nu_j + \phi_j(n)$, the correlation model complies with $E[\hat{\phi}_j(n)^* \hat{\phi}_j(\tilde{n})] = \rho\gamma$, $n \neq \tilde{n}$, and $E[\hat{\phi}_j(n)^* \hat{\phi}_j(n)] = \gamma$. This correlation model constitutes an approximation of real-life settings by assuming that all elements experience the same correlation with each other. In real-life systems, antennas farther apart from each other experience less correlation than contiguous elements. The correlation model for imperfect CSIT is given by:

$$h_j(n) = \nu + \phi_j(n) = \nu + \rho_c \hat{\phi}_j(n) + \sqrt{1-\rho_c^2} Y_j(n), \quad (4)$$

where ρ_c is the temporal correlation coefficient that describes the accuracy of the CSIT. This correlation model complies with $E[\hat{\phi}_j(n)^* \phi_j(n)] = \rho_c \gamma$. The instantaneous SINR is given by:

$$\Gamma_j = \frac{Re(P \hat{\mathbf{h}}_j^H \mathbf{h}_j)}{I_j + \sigma_v^2}, \quad (5)$$

where $I_j = \sum_{k=1}^{K} P|\delta_k h_{k,j}|^2$ is the interference created by K co-channel non-persistent interferers. Table I presents a list of the main variables used throughout this paper.

IV. Link Layer model

The probability of selection of a modulation format m is given by the probability that the estimated SNR $\hat{X}_j$ at the transmitter side lies within the interval $[\hat{\beta}_m, \hat{\beta}_{m+1}]$:

$$\Pr\{\hat{\beta}_m \leq \hat{X}_j < \hat{\beta}_{m+1}\}. \quad (6)$$

Link-layer throughput (denoted by T) will be expressed as a linear contribution of all possible MCSs with their respective selection probabilities from (6) and conditional reception probabilities, each one weighted by their conditional throughput performance (T_m):

$$T = \sum_{m=1}^{M} E_{\Gamma_{j^*}}[T_m(\Gamma_{j^*})|\hat{\beta}_m \leq \hat{X}_{j^*} < \hat{\beta}_{m+1}]$$

$$\Pr\{\hat{\beta}_m \leq \hat{X}_{j^*} < \hat{\beta}_{m+1}\}\Pr\{j^* = \arg\max_j \hat{X}_j\}, \quad (7)$$

where $T_m(\Gamma_j)$ indicates of the link-layer throughput of terminal j when using the mth MCS conditional on a given value of the operational SINR Γ_j in (5) of the selected terminal. In this paper, we consider a simplification of this expression, by assuming that the term $T_m(\Gamma)$ in (7) is a step function defined by a switching SINR threshold β_m above which all packet transmissions are assumed to be correctly received with a given BLER θ_m and spectral efficiency η_m. The simplification can be expressed as follows:

$$T = \sum_{m=1}^{M} \Delta_B W \eta_m (1-\theta_m) \Pr\{\Gamma_{j^*} \geq \beta_m|\hat{\beta}_m \leq \hat{X}_{j^*} < \hat{\beta}_{m+1}\}$$

$$\Pr\{\hat{\beta}_m \leq \hat{X}_{j^*} < \hat{\beta}_{m+1}\}\Pr\{j^* = \arg\max_j \hat{X}_j\} \quad (8)$$

where Δ_{BW} is the operational bandwidth in Hz, $\Pr\{j^* = \arg\max_j(\hat{X}_j)\}$ is the probability of terminal to experience the highest estimated SNR and therefore being scheduled for transmission by the BS, and $\Pr\{\Gamma_{j^*} \geq \beta_m|\hat{\beta}_m \leq \hat{X}_{j^*} < \hat{\beta}_{m+1}\}$ is the probability of the instantaneous SINR Γ_{j^*} to surpass the threshold β_m provided the estimated SNR $\hat{X}_{j^*}$ (used for MCS selection and terminal scheduling) lies in the range $[\hat{\beta}_m, \hat{\beta}_{m+1}]$.

Note that this last conditional probability term captures the effects of imperfect CSIT on the performance of the beamforming, scheduling and adaptation scheme. In the case of perfect CSIT ($\rho_c \to 0$), correct reception occurs with probability one. Also, note that the link-layer throughput expression in (8) represents only an approximation (compression) of the real performance of the system. The simplified model in (8) assumes packets are erroneous when the instantaneous SINR drops below the reception threshold β_m, when in practice there might be some cases where correct reception can still occur. Conversely, some cases with higher instantaneous SNR than the reception threshold could also lead to erroneous packet transmissions. This type of compression/abstraction model as in (8) has been proved accurate for system-level simulation of networks with considerable excursions of path-loss values, which are typical of cellular systems where terminals lie at different distances from the access point.

V. Performance Analysis

The following subsections present the derivation of analytic expressions of the different terms of the link-layer throughput model in (8). For convenience, it is useful to derive the statistics of the estimated SNR (presented in Section V-A) and then deal with the statistics of the instantaneous SINR (presented in Section V-C) conditional on the MCS selection, terminal scheduling, and beamforming processes.

A. Statistics of estimated SNR

Let us now substitute the correlation model described by (3) in the expression of the estimated SNR in (2), which yields:

$$\hat{X}_j = \frac{\sum_{n=1}^{N} P|\hat{h}_j(n)|^2}{\sigma_v^2} =$$

$$= \sum_{n=1}^{N} \frac{P|\nu + \sqrt{1-\rho}Z_j(n) + \sqrt{\rho}G_j|^2}{\sigma_v^2}. \quad (9)$$

The statistics of the estimated SNR have been investigated in our previous work in [37]. The sub-index j is dropped in subsequent derivations due to the symmetrical network assumption. The conditional characteristic function (CF) of $\hat{X}$ can be thus written as [39]:

$$\Psi_{\hat{X}|G}(i\omega) = (1 - i\omega\tilde{\gamma})^{-N} e^{\frac{i\omega\alpha|\tilde{\nu}+G|^2}{1-i\omega\tilde{\gamma}}}, \quad (10)$$

where $\tilde{\gamma} = \frac{P(1-\rho)\gamma}{\sigma_v^2}$, $i = \sqrt{-1}$, ω is the frequency domain variable, $\tilde{\nu} = \nu/\sqrt{\rho}$, $\alpha = \frac{PN\rho}{\sigma_v^2}$, and $\Psi_{X|Y}$ denotes the CF of random variable X conditional on an instance of random variable Y, for any X and Y random variables. By using the following change of variable $x = |\tilde{\nu} + G|^2$, the expression in (10) becomes:

$$\Psi_{\hat{X}|x}(i\omega) = (1 - i\omega\tilde{\gamma})^{-N} e^{\frac{i\omega\alpha x}{1-i\omega\tilde{\gamma}}}. \quad (11)$$

The unconditional CF of the estimated SNR can be now obtained by averaging the previous expression over the probability density function (PDF) of x, which under the Rice fading assumption is given by $f_x(x) = \sum_{q=0}^{\infty} C_q x^q e^{-\frac{x}{\gamma}}$, where $C_q = \frac{\kappa^q}{\gamma^{q+1}(q!)^2}e^{-\kappa}$ $\kappa = \frac{|\tilde{\nu}|^2}{\gamma}$ is the Rice factor. Therefore, the unconditional CF of the estimated SNR can be obtained as follows:

$$\Psi_{\hat{X}}(i\omega) = \int_0^{\infty} (1 - i\omega\tilde{\gamma})^{-N} e^{\frac{i\omega\alpha x}{1-i\omega\tilde{\gamma}}} \sum_{q=0}^{\infty} C_q x^q e^{-\frac{x}{\gamma}} dx, \quad (12)$$

which after the integration (see Appendix) becomes:

$$\Psi_{\hat{X}}(i\omega) = \sum_{q=0}^{\infty} \tilde{C}_q (1 - i\omega\breve{\gamma})^{-1-q} (1 - i\omega\tilde{\gamma})^{1+q-N}, \quad (13)$$

where $\tilde{C}_q = q! C_q \gamma^{q+1}$, $\breve{\gamma} = \alpha\gamma + \tilde{\gamma}$. The expression in (13) can be rewritten using partial fraction expansion (PFE):

$$\Psi_{\hat{X}}(i\omega) = \sum_{q=1}^{N-1} \frac{B_q}{(1 - i\omega\tilde{\gamma})^q} + \sum_{q=1}^{\infty} \frac{A_q}{(1 - i\omega\breve{\gamma})^q}. \quad (14)$$

where

$$A_q = \left\{ \begin{array}{ll} \sum_{n=1}^{N-1-q} A_{m,q}, & q \leq N-1 \\ \check{C}_q, & q > N-1 \end{array} \right. , \tag{15}$$

$$B_q = \sum_{n=0}^{N-2} B_{n,q}, \tag{16}$$

$$\check{C}_q = \sum_{w=q}^{q+N} \tilde{C}_w \sum_{t=w-q}^{N} \sum_{u=0}^{t} \left(\begin{array}{c} 1+w-N \\ t \end{array} \right) \left(\frac{\tilde{\gamma}}{\check{\gamma}}\right)^t \tag{17}$$

$$\times (-1)^{u+1} \left(\begin{array}{c} t \\ u \end{array} \right) \tag{18}$$

$$A_{q,m} = \left(\begin{array}{c} N-1-q \\ m \end{array} \right) \frac{\tilde{C}_q (-\check{\gamma})^{-1-q+m} (-\tilde{\gamma})^{1+q-N}}{(\check{\gamma}^{-1} - \tilde{\gamma}^{-1})^m}, \tag{19}$$

$$B_{q,n} = \left(\begin{array}{c} 1+q \\ n \end{array} \right) \frac{\tilde{C}_q (-\check{\gamma})^{-1-q} (-\tilde{\gamma})^{1+q-N+n}}{(\tilde{\gamma}^{-1} - \check{\gamma}^{-1})^n}. \tag{20}$$

See the Appendix for details of the derivation of these expressions. The probability density function (PDF) and complementary cumulative distribution function (CCDF) are thus given, respectively, by:

$$f_{\hat{X}}(y) = e^{-\frac{y}{\tilde{\gamma}}} \sum_{q=1}^{N-1} \frac{A_q y^{q-1}}{\tilde{\gamma}^q (q-1)!} + e^{-\frac{y}{\check{\gamma}}} \sum_{q=1}^{\infty} \frac{B_q y^{q-1}}{\check{\gamma}^q (q-1)!}, \tag{21}$$

and

$$\bar{F}_{\hat{X}}(y) = e^{-\frac{y}{\tilde{\gamma}}} \sum_{q=1}^{N-1} \sum_{m=0}^{q-1} \frac{A_q y^m}{\tilde{\gamma}^m m!} + e^{-\frac{y}{\check{\gamma}}} \sum_{q=1}^{\infty} \sum_{n=0}^{q-1} \frac{B_q y^n}{\check{\gamma}^n n!},$$

which can be rewritten, for convenience, as follows:

$$\bar{F}_{\hat{X}}(y) = e^{-\frac{y}{\tilde{\gamma}}} \sum_{q=1}^{N-1} \tilde{A}_q y^{q-1} + e^{-\frac{y}{\check{\gamma}}} \sum_{q=1}^{\infty} \tilde{B}_q y^{q-1}, \tag{22}$$

where $\tilde{A}_q = \sum_{t=q}^{N-1} \frac{A_t}{\tilde{\gamma}^{q-1}(q-1)!}$ and $\tilde{B}_q = \sum_{t=q}^{\infty} \frac{B_t}{\check{\gamma}^{q-1}(q-1)!}$.

B. Order statistics of estimated SNR

The effects of terminal scheduling on the statistics of the estimated SNR will be obtained via the theory of order statistics. The statistics of the random variable with maximum value are given by the following formula [38]:

$$f_{\hat{X}^{max}}(y) = J f_{\hat{X}}(y) F_{\hat{X}}(y)^{J-1}. \tag{23}$$

By substituting the expressions for the PDF and CDF of $\hat{X}^*$ in (23) and using the formula for multinomial theorem we obtain the following expression:

$$f_{\hat{X}^{max}}(y) = \sum_{\mathbf{l}; \sum_t l_t = J-1, q<N-1} \tilde{\alpha}_{\mathbf{l},q} e^{-y\tilde{\mu}_{\mathbf{l}}} y^{\tilde{\tau}_{\mathbf{l},q}}$$

$$+ \sum_{\mathbf{l}; \sum_t l_t = J-1, q>0} \alpha_{\mathbf{l},q} e^{-y\mu_{\mathbf{l}}} y^{\tau_{\mathbf{l},q}}, \tag{24}$$

where

$$\tilde{\alpha}_{\mathbf{l},q} = \alpha_{\mathbf{l}} \frac{\tilde{A}_q}{\tilde{\gamma}^q (q-1)!}, \tag{25}$$

$$\alpha_{\mathbf{l},q} = \alpha_{\mathbf{l}} \frac{\tilde{B}_q}{\check{\gamma}^q (q-1)!}, \tag{26}$$

$$\alpha_{\mathbf{l}} = J \left(\begin{array}{c} J-1 \\ \mathbf{l} \end{array} \right) \prod_{t=1}^{N} \left(-\tilde{A}_t\right)^{l_t} \prod_{t=N+1} \left(-\tilde{B}_{t-N+1}\right)^{l_t}, \tag{27}$$

$$\tilde{\mu}_{\mathbf{l}} = \frac{\sum_{t=1}^{N-1} l_t + 1}{\tilde{\gamma}} + \frac{\sum_{t=N} l_t}{\check{\gamma}}, \tag{28}$$

$$\tau_{\mathbf{l},q} = \sum_{t=1}^{N-1} t l_t + q - 1 + \sum_{t=N} (t-N) l_t, \tag{29}$$

$$\mu_{\mathbf{l}} = \frac{\sum_{t=1}^{N-1} l_t}{\tilde{\gamma}} + \frac{\sum_{t=N} l_t + 1}{\check{\gamma}}, \tag{30}$$

$$\tilde{\tau}_{\mathbf{l},q} = \sum_{t=1}^{N-1} (t-1) l_t + q - 1 + \sum_{t=N} (t-N) l_t. \tag{31}$$

The vector $\mathbf{l} = [l_1, l_2, \ldots l_t, \ldots]^T$ contains the exponents l_t of the elements of the multinomial term $F_{\hat{X}}(y)^{J-1}$. For details of this derivation please see the Appendix.

C. Statistics of instantaneous SINR

Let us now substitute the correlation model described by (4) into the expression of the instantaneous SINR in (5):

$$\Gamma_j = \frac{P\rho_c \hat{\mathbf{h}}_j^H \hat{\mathbf{h}}_j + Re[P \sum_{n=1}^{N} \hat{h}_j(n)^* \Phi_j(n)]}{I_j + \sigma_v^2}, \tag{32}$$

where $\Phi_j(n) = \nu(1-\rho_c) + \sqrt{1-\rho_c^2} Y_j(n)$. Since we are interested in the reception probability term $\Pr\{\Gamma_j > \beta_m\}$ we can use (32) to express the term $\Pr\{\Gamma_j > \beta_m\}$as follows:

$$\Pr\{\Gamma_j > \beta_m\} =$$

$$\Pr\left\{ \frac{P\rho_c \hat{\mathbf{h}}_j^H \hat{\mathbf{h}}_j + Re[P \sum_{n=1}^{N} \hat{h}_j(n)^* \Phi_j(n)]}{I_j + \sigma_v^2} > \beta_m \right\}.$$

By rearranging the terms of the inequality we obtain:

$$\Pr\{\Gamma_j > \beta_m\} =$$

$$\Pr\{P\rho_c \hat{\mathbf{h}}_j^H \hat{\mathbf{h}}_j + Re[P \sum_{n=1}^{N} \hat{h}_j(n)^* \Phi_j(n)] - \beta_m I_j$$

$$> \beta_m \sigma_v^2\} = \Pr\{\psi_j > \sigma_v^2\}.$$

The characteristic function of ψ_j conditionally on a particular value of $\hat{\mathbf{h}}_j$ is the addition of two random variables: a Gaussian process with mean $P\rho_c X_j + \nu(1-\rho_c)$ and variance $P(1-\rho_c)X_j = \check{\gamma} X_j$ and a non-central chi-square random variable with K degrees of freedom, and parameters $-\beta_m \lambda$ and ξ. This can be mathematically written as follows:

$$\Psi_{\psi_j|\mathbf{h}_j,k}(i\omega) = \frac{e^{i(P\rho_c X_j + \nu(1-\rho_c)) + \omega^2 \check{\gamma} X_j}}{(1+i\omega\beta_m\lambda)^K} e^{\frac{i\omega\xi^2}{1+i\omega\beta_m\lambda}}.$$

The CF conditional on the decision made by the transmitter can be obtained as follows:

$$\Psi_{\psi_j|\hat{\beta}_m<X^{max}<\hat{\beta}_{m+1},k}(i\omega) = \int_{\hat{\beta}_m}^{\hat{\beta}_{m+1}} \Psi_{\psi_j|X^*}(i\omega) f(X^{max}) dX.$$

This operation yields:

$$\Psi_{\psi_j|\hat{\beta}_m<X^{max}<\hat{\beta}_{m+1}}(i\omega) =$$

$$\sum_{\mathbf{l};\sum_t l_t=J-1;q<N-1} \frac{\tilde{\alpha}_{\mathbf{l},q}}{(i\rho_c P + \tilde{\mu}_{\mathbf{l}} + \omega^2 \tilde{\gamma})^{\tilde{\tau}_{\mathbf{l},q}+1}(1+i\omega\beta_m\lambda)^K}$$

$$\times e^{\frac{Ni\omega\xi^2}{1+i\omega\beta_m\lambda}} e^{i(1-\rho_c)\nu}$$

$$+ \sum_{\mathbf{l};\sum_t l_t=J-1,q>0} \frac{\alpha_{\mathbf{l},q}}{(i\rho_c P + \mu_{\mathbf{l}} + \omega^2 \check{\gamma})^{\tau_{\mathbf{l},q}+1}(1+i\omega\beta_m\lambda)^K}$$

$$\times e^{\frac{Ni\omega\xi^2}{1+i\omega\beta_m\lambda}} e^{i(1-\rho_c)\nu}$$

The back transform is obtained numerically thus leading to the desired statistics of instantaneous SINR

VI. Results

This section presents graphical results of the statistics of the MRC beamformer with adaptive modulation, scheduling and co-channel interference with imperfect CSIT. Figure 2 displays the results of the Cumulative Distribution Function (CDF) of the SNR of the scheduler conditional on the decision made by the transmitter based on imperfect CSIT using a hypothetical MCS selection threshold equal to ($\hat{\beta} = 2$). The results in Figure 2 have been obtained using fixed transmit power settings ($P\gamma/\sigma_v^2 = 1$) assuming no interference with different numbers of antennas ($N = 2, N = 4$), Rice factor $\kappa = -10$ dB, persistent factor $p = 0.7$, and different values of correlation coefficients ($\rho = 0.2$, $\rho = 0.95$, $\rho_c = 0.2$ and $\rho_c = 0.95$).

Figure 3 shows the results for the CDF of the SNR using the same settings as in the previous example, except for the transmit power which is now set to $P\gamma/\sigma_v^2 = 5$. The objective of investigating the conditional CDF is to observe the effects of imperfect CSIT on the instantaneous SNR experienced by the scheduled terminals. The results show the heavy influence of imperfect CSIT on the characteristics of the CDF. Low values of the correlation coefficient $\rho \to 0$, see a considerable degradation on the probability of correct reception. Note that all curves of the CDF depart from the hypothetical decision threshold set to $\hat{\beta} = 2$. This departure to the left-hand side of the figure is a measure of the incorrect reception due to imperfect CSIT. All the curves at the top left of the figure are indeed the curves with worse CSIT conditions. It is observed that spatial correlation degrades performance at high values of SNR, but it could be beneficial in the low SNR regime. In some cases, spatial diversity provided by higher numbers of antennas can even compensate for the effects of imperfect CSIT, particularly at with low values of spatial correlation. In all cases in both figures, it is observed that the performance of the CDF is superior with higher numbers of terminals in the scheduler, but this gain is more noticeable in channels with low spatial correlation. It can be also observed that user scheduling reduces the effects of spatial correlation. Spatial correlation reduces the diversity gains of the combining beamformer, and

TABLE II. SINR(dB) vs BLER FOR WiMAX MODULATION AND CODING SCHEMES [40].

QPSK 1/3		QPSK 1/2		QPSK 2/3	
SINR	**BLER**	**SINR**	**BLER**	**SINR**	**BLER**
-1.14	4.10e-3	1.32	4.13e-3	3.47	6.50e-3
QPSK 3/4		**QPSK 4/5**		**16 QAM 1/3**	
SINR	**BLER**	**SINR**	**BLER**	**SINR**	**BLER**
4.78	3.30e-3	5.46	4.97e-3	3.66	7.15e-3
16 QAM 1/2		**16 QAM 2/3**		**16 QAM 3/4**	
SINR	**BLER**	**SINR**	**BLER**	**SINR**	**BLER**
6.52	5.70e-3	9.37	3.80e-3	10.98	1.57e-3

it can be accumulated over the several antennas resulting in a more noticeable performance reduction. User scheduling provides extra diversity gains that can compensate this reduction. The results can also be compared to the Rayleigh fading case presented in our previous conference publication in [1]. All the curves seem to be more straight in the vertical direction, which is an indication of the effect of line of sight.This ”straightening” effect has consequences in different aspects of the protocol. First of all, it helps to reduce the likelihood of missing the SINR threshold for values near the threshold. However, it can also contribute to having difficulties in achieving such threshold, particularly with low values of the temporal correlation coefficient.

The results presented in Figure 3 and Figure 4 have been obtained using the same settings used in the previous two examples, except for the interference assumption. The channel power settings of the $K = 2$ persistent interferers were all set to $\lambda/\gamma = 0.1$. The results show the CDF of the instantaneous SINR instead of the SNR. The CDF results show how affected the system becomes by the presence of interference. It becomes evident that the presence of interference affects also how the spatial correlation plays a role on the performance of the system. This will become more evident in the results of throughput presented in the following figures.

To test the performance of the algorithm in a full wireless transmission system with different modulation formats, we have used the settings of the WiMAX standard and its different modulation schemes (see Table II). The results in Figure 4 and Figure 5 present the overall throughput for a network with different numbers of users included in the scheduler versus different values of transmit average SNR. Figure 4 shows the results with no interference, while Figure 5 shows the results with $K = 2$ interferers using set to $\lambda/\gamma = 0.1$. The results with interference show several changing patterns due to the complex relation between interference and the received signal by the terminals. Surprisingly at high values of transmit SNR some of the curves with low spatial correlation tend to perform worse that the correlated cases, which can only be explained by the increased importance of the interference term and the parameters of the modulation formats used in the simulation.

VII. Conclusions

This paper has presented an analytical framework for the study of joint MRC beamforming, terminal scheduling and resource allocation (modulation assignment) algorithms for multiuser networks in the presence of persistent co-channel interference. The results show that co-channel interference can

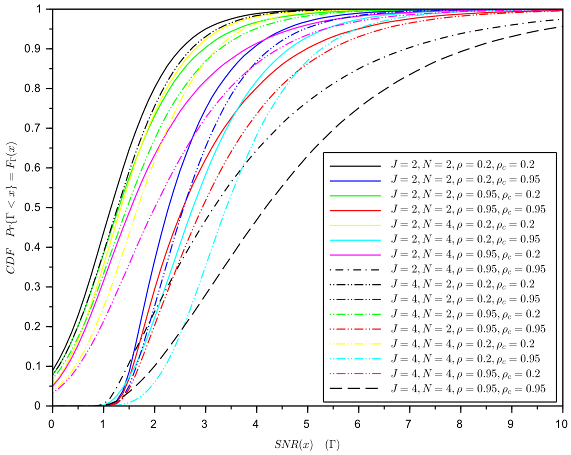

Figure 2. CDF of instantaneous SNR conditional on the estimated SNR being above the threshold $\hat{\beta} = 2$ with fixed Tx power settings $(P\gamma/\sigma_v^2) = 5)$ without interference, $\kappa = -10$ dB and different vales of antennas and correlation coefficients.

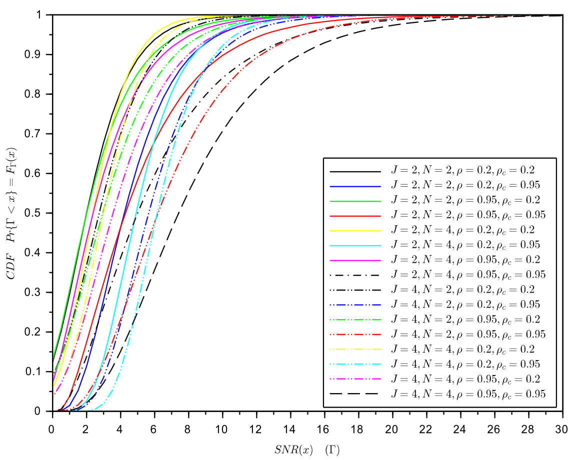

Figure 3. CDF of instantaneous SNR conditional on the estimated SNR being above the threshold $\hat{\beta} = 2$ with fixed Tx power settings $(P\gamma/\sigma_v^2) = 5)$ without interference,$\kappa = -10$ dB, and different vales of antennas and correlation coefficients.

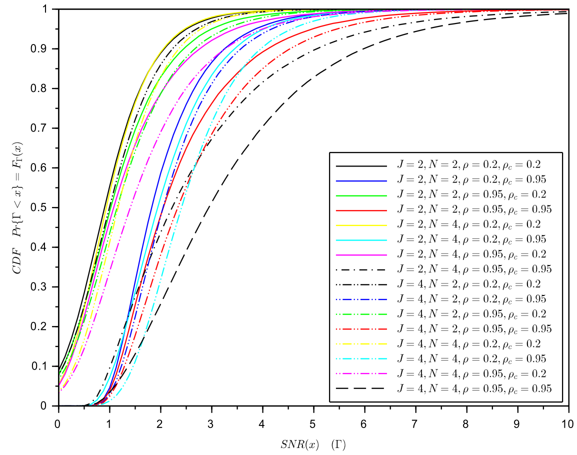

Figure 4. CDF of instantaneous SINR conditional on the estimated SNR being above the threshold $\hat{\beta} = 2$ with fixed Tx power settings $(P\gamma/\sigma_v^2) = 1)$ in the presence of cochannel interference $(K = 2, \lambda/\gamma = 0.1)$, $\kappa = -10$ dB, $p = 0.7$ and different vales of antennas and correlation coefficients.

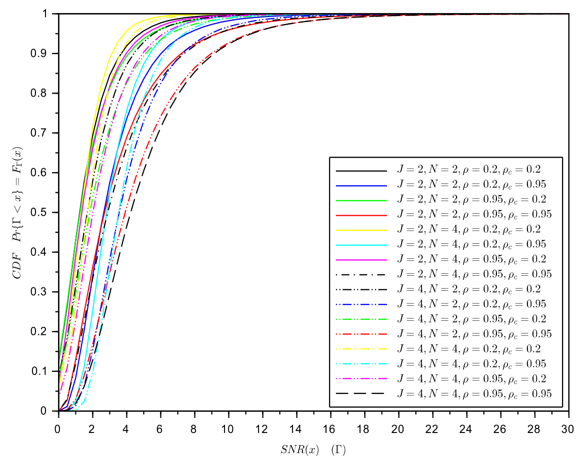

Figure 5. CDF of instantaneous SINR conditional on the estimated SNR being above the threshold $\hat{\beta} = 2$ with fixed Tx power settings $(P\gamma/\sigma_v^2) = 5)$ in the presence of co-channel interference $(K = 2, \lambda/\gamma = 0.1)$, $\kappa = -10$ dB, $p = 0.7$ and different vales of antennas and correlation coefficients.

considerably affect the performance of beamforming, being counteracted by the effects of scheduling and higher degree of accuracy of channel state information at the transmitter side. The number of antennas tends to reduce the effects of imperfect CSIT and interference. However, channel correlation can affect these gains, particularly in the high SNR regime. Conversely, in the low SNR regime it seems that channel correlation can outperform the case on uncorrelated channels. Spatial correlation effects tend to be accumulated when the number of antennas increases and, therefore, its effects will be more clearly observed in the high SNR regime. The line-of-sight component analyzed in this paper tends to improve reception for high values of temporal correlation, but it seems that when the quality of the information used for resource allocation, it contributes to reduce the diversity combining effects that can be used to overcome the errors due to imperfect CSIT.

Acknowledgments

This work has received funding from project SCOTT (www.scottproject.eu) within the Electronic Component Systems for European Leadership Joint Undertaking under grant agreement No 737422. This Joint Undertaking receives support from the European Unions Horizon 2020 research and innovation programme and Austria, Spain, Finland, Ireland,

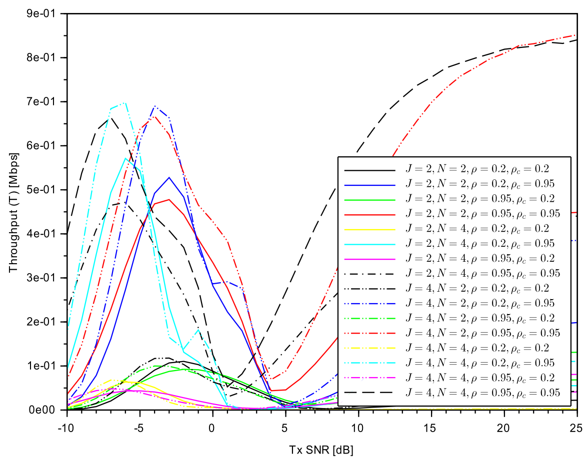

Figure 6. Throughput vs. transmit SNR for the MRC beamforming, scheduling and resource allocation algorithm without interference, $\kappa = -10$ dB and different vales of antennas and correlation coefficients.

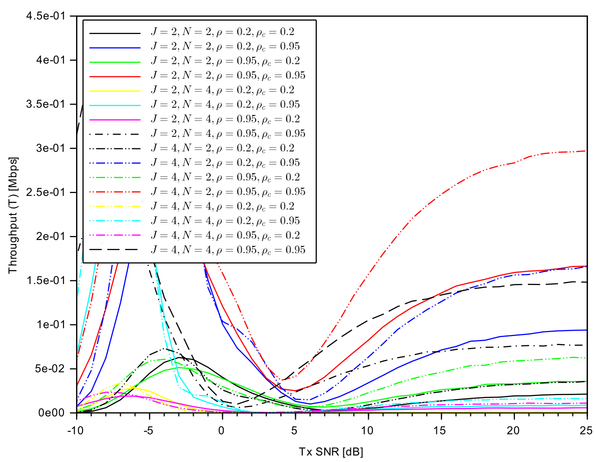

Figure 7. Throughput vs. transmit SNR for the MRC beamforming, scheduling and resource allocation algorithm in the presence of cochannel interference ($K = 2$, $\lambda/\gamma = 0.1$), $\kappa = -10$ dB, $p = 0.7$ and different vales of antennas, numbers of terminals and correlation coefficients.

Sweden, Germany, Poland, Portugal, Netherlands, Belgium, Norway. Funded also by FCT/MEC (Fundacão para a Ciência e a Tecnologia), ERDF (European Regional Development Fund) under PT2020, and by CISTER Research Unit (CEC/04234) .

Appendix

A. Derivation of the unconditional CF of $\hat{X}$ in (13)

Consider the following modification of (12):

$$\Psi_{\hat{X}}(i\omega) = \int_0^\infty (1-i\omega\tilde{\gamma})^{-N} \sum_{q=0}^\infty C_q x^q e^{-x\left(\frac{1-i\omega(\alpha\gamma+\tilde{\gamma})}{\gamma(1-i\omega\tilde{\gamma})}\right)} dx. \tag{33}$$

By using the following changes of variable $u = x\left(\frac{1-i\omega(\alpha\gamma+\tilde{\gamma})}{\gamma(1-i\omega\tilde{\gamma})}\right)$, $\breve{\gamma} = \alpha\gamma + \tilde{\gamma}$ and $du = dx\left(\frac{1-i\omega(\alpha\gamma+\tilde{\gamma})}{\gamma(1-i\omega\tilde{\gamma})}\right)$ the previous integral becomes:

$$\int_0^\infty \sum_{q=0}^\infty C_q \gamma^{q+1}(1-i\omega\tilde{\gamma})^{q+1-N}(1-i\omega\breve{\gamma})^{-1-q} u^q e^{-u} du.$$

The results of the above integration ($\int_{u=0}^\infty u^q e^{-u} du = q!$) yields the expression in (13).

B. Derivation of the partial fraction expansion of the CF of $\hat{X}$ in (14)

For convenience we rewrite the expression in (13) as follows:

$$\begin{aligned}\Psi_{\hat{X}}(i\omega) &= \sum_{q=0}^\infty \tilde{C}_q (1-i\omega\breve{\gamma})^{-1-q}(1-i\omega\tilde{\gamma})^{1+q-N} \\ &= \sum_{q=0}^{N-2} \frac{\tilde{C}_q}{(1-i\omega\breve{\gamma})^{1+q}(1-i\omega\tilde{\gamma})^{N-1-q}} \\ &\quad + \sum_{q=N-1}^\infty \frac{\tilde{C}_q (1-i\omega\tilde{\gamma})^{1+q-N}}{(1-i\omega\breve{\gamma})^{1+q}},\end{aligned} \tag{34}$$

The first term of this expression can be expanded in partial fractions as follows:

$$\frac{\tilde{C}_q}{(1-i\omega\breve{\gamma})^{1+q}(1-i\omega\tilde{\gamma})^{N-1-q}} = \sum_{m=1}^{1+q} \frac{A_{q,m}}{(1-i\omega\breve{\gamma})^m} + \sum_{n=1}^{N-1-q} \frac{B_{q,n}}{(1-i\omega\tilde{\gamma})^n},$$

where $A_{q,m} = \left(\begin{array}{c} N-1-q \\ m \end{array}\right) \frac{\tilde{C}_q(-\breve{\gamma})^{-1-q+m}(-\tilde{\gamma})^{1+q-N}}{(\breve{\gamma}^{-1}-\tilde{\gamma}^{-1})^m}$ and $B_{q,n} = \left(\begin{array}{c} 1+q \\ n \end{array}\right) \frac{\tilde{C}_q(-\breve{\gamma})^{-1-q}(-\tilde{\gamma})^{1+q-N+n}}{(\tilde{\gamma}^{-1}-\breve{\gamma}^{-1})^n}$. The second term of the expression in (34) can be rewritten as follows:

$$\sum_{q=N-1}^\infty \frac{\tilde{C}_q(1-i\omega\tilde{\gamma})^{1+q-N}}{(1-i\omega\breve{\gamma})^{1+q}} = \sum_{q=N-1}^\infty \sum_{t=0}^{1+q-N} \left(\begin{array}{c} 1+q-N \\ t \end{array}\right) \frac{\tilde{C}_q(-i\omega\tilde{\gamma})^t}{(1-i\omega\breve{\gamma})^{1+q}},$$

which can be rewritten as

$$\begin{aligned}&\sum_{q=N-1}^\infty \sum_{t=0}^{1+q-N} \left(\begin{array}{c} 1+q-N \\ t \end{array}\right) \sum_{u=0}^{t} \left(\begin{array}{c} t \\ u \end{array}\right) \\ &\qquad \times \frac{\tilde{C}_q(\tilde{\gamma}/\breve{\gamma})^t(-1)^{u+1}}{(1-i\omega\breve{\gamma})^{1+q-u}} \\ &\quad = \sum_{q=N-1}^\infty \frac{\breve{C}_q}{(1-i\omega\breve{\gamma})^{1+q}},\end{aligned}$$

where

$$\begin{aligned}\breve{C}_q = \sum_{w=q}^{q+N} \tilde{C}_w \sum_{t=w-q}^{N} \sum_{u=0}^{t} \left(\begin{array}{c} 1+w-N \\ t \end{array}\right) \left(\frac{\tilde{\gamma}}{\breve{\gamma}}\right)^t \\ \times (-1)^{u+1} \left(\begin{array}{c} t \\ u \end{array}\right).\end{aligned}$$

By substituting the results back in (34), we obtain:

$$\Psi_{\hat{X}}(i\omega) = \sum_{q=0}^{N-2}\left\{\sum_{m=1}^{1+q}\frac{A_{q,m}}{(1-i\omega\breve{\gamma})^m} + \sum_{n=1}^{N-1-q}\frac{B_{q,n}}{(1-i\omega\tilde{\gamma})^n}\right\} + \sum_{q=N-1}^{\infty}\frac{\breve{C}_q}{(1-i\omega\breve{\gamma})^{1+q}},$$

which can be rewritten as

$$\Psi_{\hat{X}}(i\omega) = \sum_{q=1}^{N-1}\frac{B_q}{(1-i\omega\tilde{\gamma})^q} + \sum_{q=1}^{\infty}\frac{A_q}{(1-i\omega\breve{\gamma})^q},$$

where: $A_q = \begin{cases} \sum_{n=1}^{N-1-q} A_{m,q}, & q \leq N-1 \\ \breve{C}_q, & q > N-1 \end{cases}$, and $B_q = \sum_{n=0}^{N-2} B_{n,q}$,

C. Derivation of order statistics of estimated SNR in from (2)

Using the multinomial theorem, it is possible to obtain a formula for the term $F_{\hat{X}}(y)^{J-1}$ considering the expression in (22) as follows:

$$F_{\hat{X}}(y)^{J-1} = \sum_{\sum_t l_t = J-1}\begin{pmatrix} J-1 \\ \mathbf{l}\end{pmatrix}\prod_{t=1}^{N-1}\left(-\tilde{A}_t y^{t-1} e^{-\frac{y}{\tilde{\gamma}}}\right)^{l_t} \times \prod_{t=N}\left(-\tilde{B}_{t-N+1} y^{t-N} e^{-\frac{y}{\breve{\gamma}}}\right)^{l_t}$$

where l_t is the exponent index of the t-th element of the multinomial expression$(x_0 + x_1 + x_2 + \ldots x_t + x_{t+1}\ldots)^{J-1}$, considering that $x_0 = 1$, $x_t = -\tilde{A}_t y^{t-1} e^{-\frac{y}{\tilde{\gamma}}}$, $1 \leq t \leq N-1$, $x_t = -\tilde{B}_{t-N+1} y^{t-N} e^{-\frac{y}{\breve{\gamma}}}$, $N \leq t$,. The vector $\mathbf{l} = [l_1, l_2, \ldots l_t, \ldots]^T$ contains the exponents l_t of the elements of the multinomial term $F_{\hat{X}}(y)^{J-1}$. The previous expression can be reorganized as follows:

$$F_{\hat{X}}(y)^{J-1} = \sum_{\sum_t l_t = J-1}\begin{pmatrix} J-1 \\ \mathbf{l}\end{pmatrix} \times e^{-y\left(\frac{\sum_{t=1}^{N-1} l_t}{\tilde{\gamma}} + \frac{\sum_{t=N} l_t}{\breve{\gamma}}\right)} y^{\sum_{t=1}^{N-1}(t-1)l_t + \sum_{t=N}(t-N)l_t} \times \prod_{t=1}^{N}\left(-\tilde{A}_t\right)^{l_t}\prod_{t=N+1}\left(-\tilde{B}_{t-N+1}\right)^{l_t}$$

By substituting the previous expression back in (23) we then obtain:

$$f_{\hat{X}^{max}}(y) = \sum_{\sum_t l_t = J-1}\begin{pmatrix} J-1 \\ \mathbf{l}\end{pmatrix} \times e^{-y\left(\frac{\sum_{t=1}^{N-1} l_t}{\tilde{\gamma}} + \frac{\sum_{t=N} l_t}{\breve{\gamma}}\right)} y^{\sum_{t=1}^{N-1}(t-1)l_t + \sum_{t=N}(t-N)l_t} \times \prod_{t=1}^{N}\left(-\tilde{A}_t\right)^{l_t}\prod_{t=N+1}\left(-\tilde{B}_{t-N+1}\right)^{l_t} \times \left(e^{-\frac{y}{\tilde{\gamma}}}\sum_{q=1}^{N-1}\frac{\tilde{A}_q y^{q-1}}{\tilde{\gamma}^q (q-1)!} + e^{-\frac{y}{\breve{\gamma}}}\sum_{q=1}^{\infty}\frac{\tilde{B}_q y^{q-1}}{\breve{\gamma}^q (q-1)!}\right),$$

which can be rewritten as follows

$$f_{\hat{X}^{max}}(y) = \sum_{\sum_t l_t = J-1}\alpha_{\mathbf{l}} e^{-y\left(\frac{\sum_{t=1}^{N-1} l_t}{\tilde{\gamma}} + \frac{\sum_{t=N} l_t}{\breve{\gamma}}\right)} \times y^{\sum_{t=1}^{N-1}(t-1)l_t + \sum_{t=N}(t-N)l_t} \times \left(e^{-\frac{y}{\tilde{\gamma}}}\sum_{q=1}^{N-1}\frac{\tilde{A}_q y^{q-1}}{\tilde{\gamma}^q (q-1)!} + e^{-\frac{y}{\breve{\gamma}}}\sum_{q=1}^{\infty}\frac{\tilde{B}_q y^{q-1}}{\breve{\gamma}^q (q-1)!}\right)$$

where

$$\alpha_{\mathbf{l}} = J\begin{pmatrix} J-1 \\ \mathbf{l}\end{pmatrix}\prod_{t=1}^{N}\left(-\tilde{A}_t\right)^{l_t}\prod_{t=N+1}\left(-\tilde{B}_{t-N+1}\right)^{l_t}.$$

A further modification of this expression leads to:

$$f_{\hat{X}^{max}}(y) = \sum_{\mathbf{l};\sum_t l_t = J-1}\sum_{q=1}^{N-1}\tilde{\alpha}_{\mathbf{l},q} e^{-y\left(\frac{\sum_{t=1}^{N-1} l_t + 1}{\tilde{\gamma}} + \frac{\sum_{t=N} l_t}{\breve{\gamma}}\right)} \times y^{\sum_{t=1}^{N-1}(t-1)l_t + q - 1 + \sum_{t=N}(t-N)l_t}$$
$$+ \sum_{\mathbf{l};\sum_t l_t = J-1}\sum_{q=1}^{\infty}\alpha_{\mathbf{l},q} e^{-y\left(\frac{\sum_{t=1}^{N-1} l_t}{\tilde{\gamma}} + \frac{\sum_{t=N} l_t}{\breve{\gamma}}\right)} \times y^{\sum_{t=1}^{N-1} t l_t + \sum_{t=N}(t-N)l_t + q - 1}$$

where

$$\tilde{\alpha}_{\mathbf{l},q} = \alpha_{\mathbf{l}}\frac{\tilde{A}_q}{\tilde{\gamma}^q (q-1)!},$$

and

$$\alpha_{\mathbf{l},q} = \alpha_{\mathbf{l}}\frac{\tilde{B}_q}{\breve{\gamma}^q (q-1)!}.$$

This can be rewritten as the intended expression in (24), which finalizes the derivation.

References

[1] R. Samano-Robles, "Joint Beamforming, Terminal Scheduling, and Adaptive Modulation with Imperfect CSIT in Rayleigh Fading Correlated Channels with Co-channel Interference," *The Second International Conference on Advances in Signal, Image and Video Processing - from Sensing to Applications (SIGNAL 2017)*. 21-25 May 2017, 5GSIGNAL-WAVE. Barcelona, Spain.

[2] H. Kim, "Coding and modulation techniques for high spectral efficiency transmission in 5G and Satcom," *23rd European Signal Processing Conference (EUSIPCO)* Nice, France, pp. 2746-2750, 31 Aug.-4 Sept. 2015, DOI: 10.1109/EUSIPCO.2015.7362884

[3] A. Goldsmith, S. A. Jafar, N. Jindal, and S. Vishwanath, "Capacity limits of MIMO channels," *IEEE Journal on Selected Areas in Communications*, vol. 21, no. 5, pp. 684-702, June 2003, DOI: 10.1109/JSAC.2003.810294

[4] W. Ge, J. Zhang, and G. Xue, "MIMO-Pipe Modeling and Scheduling for Efficient Interference Management in Multihop MIMO Networks," *IEEE Transactions on Vehicular Technology,* vol. 59, no. 8, pp. 3966-3978, Oct. 2010, DOI: 10.1109/TVT.2010.2060376

[5] R. Smano-Robles and A. Gameiro, "Joint Scheduling, link adaptation and space division multiplexing for distributed antenna systems," *TELFOR (Telecommunications Forum)* Belgrade, Serbia, 2012.

[6] D. Soldani and A. Mazalini, "On the 5G Operating System for a True Digital Society," *IEEE Vehicular Technology Magazine. 2015* March, pp. 32-42. DOI: 10.1109/MVT.2014.2380581

[7] A. Sasi and P. Santhiva, "Quantum internet using 5G NanoCore with Beam Division Multiple Access," *International Conference on Advanced Computing and Communication Systems*, Jan. 2015, Coimbatore, India, 2015.

[8] H. J. Yang,W.-Y. Shin, B. C. Jung, C. Suh, and A. Paulraj, "Opportunistic Downlink Interference Alignment for Multi-Cell MIMO Networks," *IEEE Transactions on Wireless Communications.* vol. 16, no. 3, pp. 1533 - 1548, March 2017, DOI: 10.1109/TWC.2017.2647942

[9] F. Rashid, K. J. Ray Liu, and L. Tassiulas, "Transmit beamforming and power control for cellular wireless systems," *IEEE Journal on Selected Areas in Communications,* vol. 16, no. 8, pp. 1437-1450, Oct. 1998, DOI: 10.1109/49.730452

[10] H. Dahrouj and W. Yu. "Coordinated beamforming for the multi-cell multi-antenna wireless system," *IEEE Transactions on Wireless Communications,* vol. 9, no. 5, pp. 1748-1759, May 2010, DOI: 10.1109/TWC.2010.05.090936.

[11] Y. Huang, G. Zheng, M. Bengtsson, K. Wong, L. Yang, and B. Ottersten, "Distributed Multicell Beamforming With Limited Intercell Coordination," *IEEE Transactions on Signal Processing,* vol. 59, no. 2, pp. 728-738, Feb. 2011, DOI: 10.1109/TSP.2010.2089621

[12] Deliverable D5.1: System level evaluation metrics and interfacing, "FP7 CODIV: Enhanced Wireless Communication Systems Employing COoperative DIVersity,", Available at: http://www.ict-codiv.eu/ Last Accessed November 2017.

[13] Deliverable D5.4: Final report on link level and system level channel models, "FP7 WINNER: Wireless World Initiative New Radio,", Available at: http://www.ist-winner.org Last Accessed November 2017.

[14] Deliverable D7.1: System level interfacing, metrics and simulation scenarios, "FP7 FUTON: Fibre-Optic Networks for Distributed Extendible Heterogeneous Radio Architectures and Service,", Available at: http://www.ict-futon.eu/ Last Accessed November 2017.

[15] K. Brueninghaus, et al., "Link performance model models for system level simulations of broadband radio access systems," *Proceedings IEEE International Symposium on Personal, Indoor and Mobile Radio Communications*, vol. 4, pp. 2306-2311, March 2005.

[16] J. Murkovic, G. Orfanos, and H. J. Reumermann, "MIMO link modeling for system-level simulations," *The 17th annual IEEE International Symposium on Personal, Indoor and Mobile Radio Communications, PMRC,* , vol. 4, pp. 1-6, 2006.

[17] M. Wrulich and M. Rupp, "Efficient link measurement model for system-level simulations of Alamouti encoded MIMO HSDPA transmissions," *2008 ITG Workshop on smart antennas* pp. 351-355.

[18] A. Perez-Niera and M Campalans, "Cross-Layer Resource Allocation in Wireless Communications: Techniques and Models from PHY and MAC Layer Interaction," *Academic Press, Oxford, 2010*

[19] F. A. Dietrich and W. Utschick, "Maximum ratio combining of correlated Rayleigh fading channels with imperfect channel knowledge," *IEEE Communications Letters*, vol. 7, no. 9, pp. 419-421, Sept. 2003, DOI: 10.1109/LCOMM.2003.817299.

[20] Y. Ma, R. Schober, and S. Pasupathy, "Effect of channel estimation errors on MRC diversity in Rician fading channels," *IEEE Trans. on Vehicular Technologies*, vol. 54, no. 6, pp. 2137-2142, November 2005, DOI: 10.1109/TVT.2005.853454.

[21] Y. Ma, "Impact of correlated diversity branches in Rician fading channels," *IEEE International Conference on Communications (ICC)*, vol. 1, pp. 473-477, 2005.

[22] H. T. Hui, "The performance of the maximum ratio combining method in correlated Rician-Fading channels for antenna-diversity signal combining," *IEEE Trans. on Antennas and Propagation*, vol. 53, no. 3, pp. 958-964, March 2005, DOI: 10.1109/TAP.2004.842649.

[23] P. Loskot and N.C. Beaulieu, "A unified approach to computing error probabilities of diversity combining schemes over correlated fading channels," *IEEE Transactions on Communications*, vol. 57, no. 7, pp. 2031-2041, 2009.

[24] N.C. Beauliu and X. Zhang, "On selecting the number of receiver diversity antennas in Ricean fading cochannel interference," *IEEE Global Telecommunications Conference (Globecom) 2006*, pp. 1-6.

[25] N.C. Beauliu and X. Zhang, "On the maximum number of receiver diversity antennas that can be usefully deployed in a cochannel interference dominated environment," *IEEE Transactions on Signal Processing*, vol. 55, no. 7, pp. 3349-3359, July 2007, DOI: 10.1109/TSP.2007.894395.

[26] N.C. Beauliu and X. Zhang, "On the maximum useful number of receiver antennas for MRC diversity in cochannel interference and noise," *IEEE International Conference on Communications (ICC)*,pp. 5103-5108.

[27] K. S. Ahn and R.W. Heath, "Performance analysis of maximum ratio combining with imperfect channel estimation in the presence of cochannel interferences," *IEEE Transactions on Wireless Communications*, vol. 8, no. 3, pp. 1080-1085, March 2009, DOI: 10.1109/TWC.2009.080114.

[28] R. Samano-Robles and A. Gameiro, "Joint Spectrum Selection and Radio Resource Management for Distributed Antenna Systems with Cognitive Radio and Space Division Multiplexing," *Workshop on Smart Antennas, Stuttgart, Germany,* 2013.

[29] L.Chen, Y. Yang, X. Chen, and G. Wei, "Energy-Efficient Link Adaptation on Rayleigh Fading Channel for OSTBC MIMO System With Imperfect CSIT," *IEEE Transactions on Vehicular Technology*, vol. 62, no. 4, pp. 1577-1585, May 2013, DOI: 10.1109/TVT.2012.2234155.

[30] A. E. Ekpenyong and Y.F. Huang, "Feedback Constraints for Adaptive Transmission," *IEEE Signal Processing Magazine*, vol. 24, no. 3, pp. 69-78, May 2007, DOI: 10.1109/MSP.2007.361603.

[31] S.i Zhou and G. B. Giannakis, "Adaptive Modulation for Multi-antenna Transmissions With Channel Mean Feedback," *IEEE Transactions on Wireless Communications*, vol. 3, no. 5, pp. 1626-36, Sept. 2004, DOI: 10.1109/TWC.2004.833411.

[32] M. Torabi and J.F. Frigon, "Impact of Outdated Feedback on the Performance of M-QAM Adaptive Modulation in User Selection Diversity Systems with OSTBC over MIMO Rayleigh Fading Channel," *IEEE Vehicular Technology Conference,* 3-6 Sept. 2012, Canada.

[33] P. Yang, Y. Xiao, Y. Yu, L. Li, Q. Tang, and S. Li, "Simplied Adaptive Spatial Modulation for Limited-Feedback MIMO Systems," *IEEE Signal Processing Magazine*, vol. 62, no. 6, pp. 2656 - 2666, July 2013, DOI: 10.1109/TVT.2013.2242502.

[34] P. Xia, S. Zhou, and G. B. Giannakis, "Multiantenna Adaptive Modulation With Beamforming Based on Bandwidth Constrained Feedback," *IEEE Transactions on Communications* vol. 53, no. 3, pp. 526 - 536, March 2005, DOI: 10.1109/TCOMM.2005.843431.

[35] Z. Bouida, A. Ghrayeb, and K. A. Qaraqe, "Adaptive Spatial Modulation for Spectrum Sharing Systems With Limited Feedback," *IEEE Transactions on Communications,* vol. 63, no. 6, pp. 2001-2014, June 2015, DOI: 10.1109/TCOMM.2015.2420567.

[36] Z. Bouida, A. Ghrayeb, and K. A. Qaraqe, "Joint Adaptive Spatial Modulation and Power Adaptation for Spectrum Sharing Systems with Limited feedback," *IEEE Wireless Communications and Networking Conference (WCNC 2015)*

[37] R. Samano Robles, E. Lavendelis, and E. Tovar, "Performance Analysis of MRC Receivers with Adaptive Modulation and Coding in Rayleigh Fading Correlated Channels with Imperfect CSIT," *Wireless Communications and Mobile Computing*, Volume 2017 (2017), Article ID 6940368,.

[38] http://mathworld.wolfram.com/OrderStatistic.html

[39] J. Proakis, *Digital Communications,* McGraw-Hill, 4th edition 2001.

[40] WiMAX Forum Standard,"*WiMAX system level evaluation methodology, V.0.0.1,*" 2006.